Collection of Gaseous and Aerosolized Samples Using Microfluidic Devices With Gas–Liquid Interfaces

Jason D. Greenwood, Ye Liu, *Student Member, IEEE*, David E. Busacker, Daming Cheng, and Hongrui Jiang, *Senior Member, IEEE*

Abstract—We demonstrated methods for collecting gaseous samples and aerosolized particles into microfluidic channels. Gas–liquid interfaces created by surface tension permit analytes to transfer from the environment into a microfluidic channel. In one structure of our design, hydrophobic–hydrophilic boundaries created a channel of liquid confined by gas–liquid interfaces in which analytes were collected. In another structure, circular air pillars within microfluidic channels were created by surface tension forces for analytes collection. A multileveled structure could be formed by the air pillar design with a simple process, enabling it to collect and separate multiple analytes at a time. Both structures were tested with ammonia as a gaseous sample and Kool-Aid as aerosolized particles. The sample acquisition capabilities of the devices were demonstrated by extensive testing with gaseous NH_3, using Nessler's reagent as the collecting fluidic stream, and with aerosolized Kool-Aid particles, using deionized (DI) water as the collecting fluidic stream. Increasing the exposed fluidic surface area to the environment effectively increased collection efficiency of the devices. This was confirmed by a resistance study between different sets of designs of both structures. Real-time analysis potential was also demonstrated through measurement of DI water resistance by collecting varying concentrations of gaseous NH_3.

Index Terms—Aerosolized sample collection, air pillars, gas–liquid interface, microfluidics.

I. INTRODUCTION

COLLECTION and real-time monitoring of airborne and gaseous samples such as explosives, drugs, dioxins, and bacteria have become an important issue for homeland secu-

rity, air pollution monitoring, and medical diagnosis [1]–[3]. Although the substance of interest is usually airborne, analysis of liquid aggregates is the most common method for chemical and biology analysis. As a result, sample to liquid interfacing is demonstrated to be an efficient method of collecting and delivering gaseous samples and aerosolized particles and also shows the potential to be a part of certain diagnosis systems, e.g., to observe ammonia levels in air exhaled by the patient [4], and to be a part of chemical/biological sensors, e.g., to acquire toxic bacterial spore particles by dissolving them in a liquid [5]. To enable gas–liquid interactions, capillary action [6] and surface chemistry [1] have been utilized previously. Sridharamurthy and Jiang reported an interesting surface-tension-held gas-liquid interface pinned at hydrophilic–hydrophobic polymer–glass interface for sample collection with a relatively simple fabrication process [7]. Although these methods are effective and point out the direction for novel designs, there still exist issues such as requirement of relatively complicated fabrication processes or polymer swelling problems during operation. We previously presented a preliminary study of the method of creating microfluidic channel with gas–liquid interface by hydrophobic self-assembled monolayer (SAM) on gold surfaces [8]. Here, we present an expanded study of such devices (called channel devices) and recently developed air pillar devices utilizing relatively simple fabrication processes and low-cost materials while showing good collecting performance.

Gas–liquid interfaces can be created using various methods. One prevailing method is to create hydrophobic–hydrophilic interfaces so aqueous liquids can be pinned by surface tension at the interfaces [9], [10]. Current processes for creating such hydrophobic–hydrophilic interfaces usually involves the usage of octadecyltrichlorosilane (OTS) to create an SAM on the glass surface [11], [12], which is relatively complicated [13]. This complication in hydrophobic surface formation requires additional consideration in device design and fabrication. A previous study of our group has demonstrated that patterned isobornyl acrylate (IBA) is an easier and more efficient way to create the hydrophobic–hydrophilic boundary [7]. However, IBA might swell when interacting with certain solvents, limiting the lifetime of the devices and introducing uncertainties during their operation.

To overcome this problem, we have demonstrated gas–liquid interface channel devices in which the hydrophilic–hydrophobic interfaces are formed by the self-assembly of alkanethiol monolayers on gold surface, instead of IBA. Comparing to previous devices created by flushing OTS into complicated microfluidic networks [14], our channel devices have simpler fabrication pro-
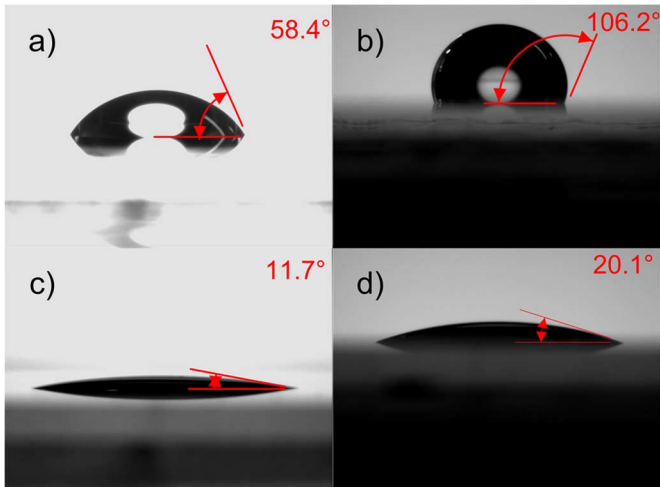
Fig. 1. Contact angle profile of a droplet on alkanethiol-treated gold (b) and glass slide surfaces (d) with comparison to untreated surfaces (a), (c). The profile pictures are taken with a goniometer.
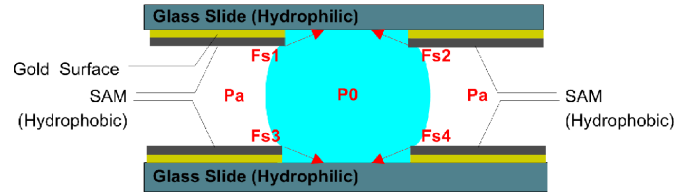

Fig. 2. Diagram showing the forces involved in the hydrophobic–hydrophilic boundaries. The liquid is held in the channel by the surface tension of the liquid (F_{s1}, F_{s2}, F_{s3}, and F_{s4}) due to the abrupt wettability change at the Au–glass interface.
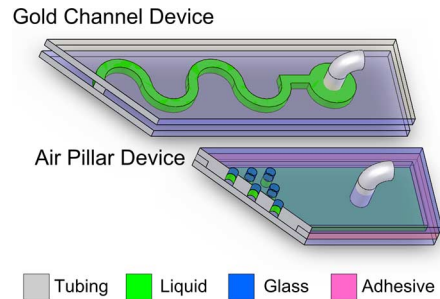

Fig. 3. Three-dimensional rendition of a channel device (top) and an air pillar device (bottom).

cedures and better compatibility with lab-on-a-chip applications since only gold and glass have been used as the bulk material.

The SAM worn out on the device might be a concern for such device. To eliminate the need of SAM and prolong the device shelf life, we reveal an alternative way to form the hydrophilic–hydrophobic interface by constructing air pillar structures from predrilled holes in glass pinning the liquid at interface. For such devices, the fabrication process is straightforward, very low cost, and showed improvement of robustness and performance over other comparable designs. We also demonstrated multilevel air pillar devices with a relatively simple fabrication process, in which each level could be occupied by a specific collecting liquid stream. This design allows for multiple streams to be simultaneously exposed to the environment. Each stream could potentially contain agents (e.g., antibodies) that specifically bind with one type of gaseous/aerosolized analyte, while other analytes unbound are flushed away. Therefore, this design could realize not only sample collection but also sample constituent separation and would be of great benefit to high-throughput detection.

II. PRINCIPLES OF OPERATION

A. Formation of Hydrophobic–Hydrophilic Interfaces

Hydrophobic SAM of alkanethiol formed on the surface of a copper or gold layer has been reported [15], [16], and such monolayer hardly forms on a glass surface, which has been further demonstrated in Fig. 1. Hence, the wettability will change abruptly at the interface of an alkanethiol-treated gold surface and a treated glass surface, thus forming a hydrophobic–hydrophilic boundary. Utilizing this method, two gold-coated glass slides with patterned gold films and alkanethiol treatment are aligned and stacked "face to face" to form our channel device, as shown in Fig. 2. The glass slides are separated by adhesive tape spacers by ∼60 μm at the corners with no confinement at the lateral and transverse directions. When an aqueous liquid is flowed through, the surface tension will balance the pressure difference between the liquid and the atmosphere and pin the lateral surface of the fluid stream at the

glass–gold hydrophilic–hydrophobic interface. As a result, the liquid stream is confined in the glass section of the surfaces of the slides by a "wall" of surface tension as long as the pressure difference does not exceed a critical value, and the airborne analytes can enter the device from the lateral direction and be collected dynamically by the fluid stream.

B. Air Pillar Structures for Airborne Analyte Collection

A glass microscope slide with predrilled hole-pattern, an inlet, and an outlet is stacked on top of another patterned or unpatterned slide to form a single-level air pillar device, as shown in Fig. 3 (bottom), and the transverse and lateral directions are sealed by adhesive tapes. Air pillars can be formed with holes predrilled only on the top surface of the channel (i.e., the single level air pillar structure, case I), or with through holes predrilled on both the top and bottom of the glass surface (corresponding to one level in a multilevel air pillar device, case II). Fig. 4(a)–(c) depicts the formation of air pillars in case I, while Fig. 4(d)–(f) illustrates the formation of air pillars in case II. In both cases, according to Young–Laplace equation [10], [17], we have

$$\Delta P = P_1 - P_0 = \gamma_{LG}\left(\frac{1}{r} + \frac{1}{R}\right) \qquad (1)$$

where r and R are the radii of curvature in directions vertical and parallel to the liquid stream, and γLG is the surface tension. The dimension along the boundary is much larger than the channel height in our microfluidic devices. Thus, (1) is reduced to (h is the height of the channel)

$$P_1 - P_0 = \frac{\gamma_{\mathrm{LG}}}{r}, \qquad \text{where} \quad r = \frac{h}{2\cos(180° - \theta_1)}$$

hence

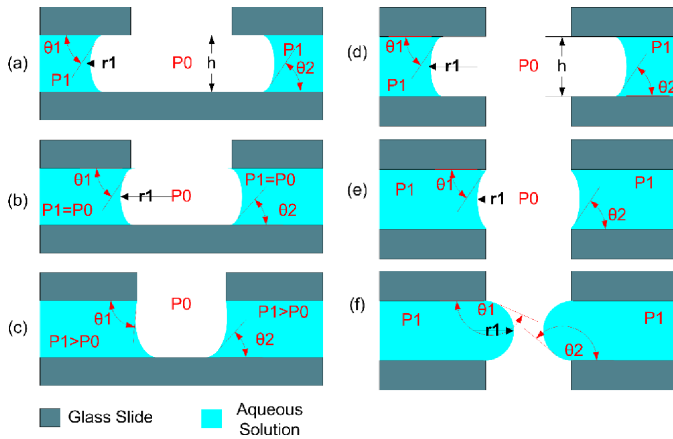$$P - P_0 = \frac{2\gamma_{LG}}{h}\cos(180° - \theta_1). \qquad (2)$$

Fig. 4. (a)–(c) Formation of air pillars with device structure in case I, (d)–(f) formation of air pillars with device structure in case II. In (a) and (d), aqueous solution is still in the hydrophilic area; the liquid–air interface will maintain the same shape and move forward until arriving at the hole boundary. The pressure in the aqueous solution remains the same P_1. When the liquid–air interface arrives at the hole, it is pinned by the rough edge [see (b) and (e)]. When the pressure of the aqueous solution increases, the interface will assume different shape. In case I, contact angle θ_2 still approximately equals to the contact angle formed by a drop of the same aqueous solution on the same hydrophilic glass surface, while θ_1 can change continuously until the air pillar is filled (c). In case II, both θ_1 and θ_2 will change, because the interface is pinned at both the top and bottom hydrophobic–hydrophilic boundaries, thus changing the meniscus of the liquid–air interface from concave ($r < 0$), to flat ($r = \infty$), and eventually to convex ($r > 0$) (f).

In both cases, when an aqueous liquid is flowed in the channel [see Fig. 4(a) and (d)] but has not reached the hole, the liquid–air interface forms a meniscus with a fixed contact angle at the top and bottom surfaces of the channel θ_1, which is equal to the contact angle formed by a drop of the same aqueous solution on the same hydrophilic glass surface [10]. Because in the hydrophilic side of the channel $\theta_1 < 90°$, r_1 is negative, and P_1 is smaller than P_0. Therefore, the liquid–air interface moves toward the hydrophobic–hydrophilic boundary with a fixed shape of meniscus.

In both cases, after the aqueous liquid arrives at a boundary of a hole, the liquid–air interface is pinned by the rough edge of the hole. In case I, only the top contact line of the interface is pinned. In case II, both contact lines of the liquid–air interface with the top and bottom surfaces of the channel are pinned [see Fig. 4(b) and (e)].

In case I, keeping increasing the fluid pressure (by introducing the aqueous solution in the channel) has very little affect on the contact angle at the free contact line θ_2. Since the bottom contact line of the interface is not pinned, the meniscus will always remain concave [see Fig. 4(c)]. In case II, however, increase in the fluid pressure will introduce change in both θ_1 and θ_2, because the interface is pinned at both the top and bottom contact lines, thus changing the meniscus of the liquid–air interface from concave ($r < 0$), to flat ($r = \infty$), and eventually to convex ($r > 0$) [see Fig. 4(f)]. According to previous study in [18], the contact angle between the liquid–air interface and the channel surface θ increases from $\theta_{1,2}$ to θ_{max}, where θ_{max} is the maximum contact angle that can be sustained by the boundary. To our observation, θ_{max} is related to both the interfacial energy of the solid surface contacting the aqueous solution and
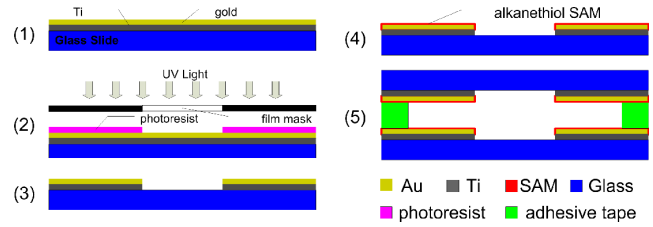

Fig. 5. Fabrication process of the channel device. (a) Au–Ti coated glass slide. (b) Single mask photolithography to define the geometry of the gas–liquid interface and the channel. (c) Etching Au and Ti, then removing photoresist. (d) SAM surface treatment. (e) Bonding two slides "face to face" together using adhesive tape at each corner of the slides.

the roughness of the edge. Further increase in the liquid pressure will result in a large pressure difference that breaks the force balance at the pinned surface. As a result, the air pillars will disappear in both cases.

III. DEVICE FABRICATION

A. Channel Device With Hydrophobic–Hydrophilic Interface

As shown in Fig. 5, microscope slides precoated with Ti and Au (50 and 1000 Å, respectively) were obtained from Evaporated Metal Films, Inc. (Ithaca, NY). A single-mask photolithography process was then preformed to pattern the Au–Ti film on the glass slide using positive photoresist (AZ4620, Shipley Company, LLC, Marlborough, MA). The exposed gold layer was removed with gold etchant, and then a short submersion in hydrofluoric acid removed the thin Ti layer, exposing the glass surface. This defined the channel geometry, which in our experiment is serpentine (larger gas–liquid interface area) or straight (smaller area). The process was repeated to obtain another Au–Ti coated microscope slide with an identical pattern. Through holes were drilled into one of the two slides at opposing ends of the channel as the inlet and outlet. Both slides were then placed in a solution of 1-mM hexadecanethiol (Acros Organics, Fair Lawn, NJ) diluted with 200 mL of ethanol for 2 h. They were then rinsed with ethanol and allowed to dry, forming a hydrophobic SAM layer on top of the Au [see Fig. 5 (d)]. Finally, the two slides are aligned and bonded using 60-μm-thick double-sided adhesive tape (3M, St. Paul, MN), forming the final device.

B. Single- and Multilevel Air Pillar Devices

For a single-level air pillar device, through holes are drilled on the top glass microscope slide, forming a specific hole pattern. Inlet and outlet holes were drilled on opposing ends of the pattern and connected with ethyl vinyl acetate microbore tubing. The patterned slide was bonded to another clean microscope slide (hole-patterned or not patterned) using double-sided adhesive tape of a desired thickness (3M, St. Paul, MN), forming a channel.

For a multilevel air pillar device, an identical through-hole pattern was drilled into two or more slides. Inlet and outlet holes were drilled at arbitrary locations on opposing ends of each hole-patterned slide. Tubing was inserted for open access to each level. The patterned slides were aligned vertically and bonded to another clean microscope slide, using double-sided
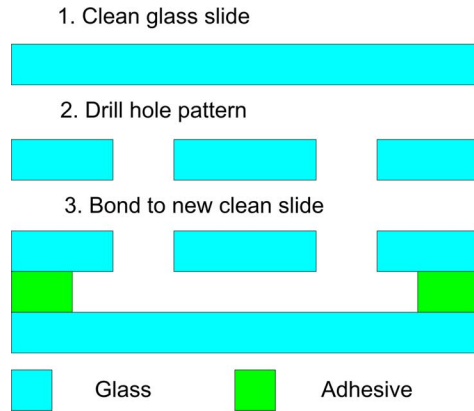
Fig. 6. Fabrication of a multilevel air pillar device. (a) Inspect glass slides for defects. (b) Drill-aligned hole patterns in glass slides. (c) Stack, align, and bond hole-patterned glass slides to a new clean slide, using double-sided adhesive tape to create the device.

adhesive tape with a desired thickness (3M, St. Paul, MN), forming channels at each level (see Fig. 6).

IV. DESIGN CONSIDERATIONS

For air pillar devices, different hole patterns were considered before the final layout was chosen. Fig. 7 shows the flow and pressure analysis of two different layout methods: aligned "hole matrix" [see Fig. 7(a) and (b)] and offsetting hole arrays [see Fig. 7(c) and (d)]. The simulation creates a simplified 2-D model for the collecting fluid level with air pillars with exactly the same dimensions as the device. We use FLUID141 (2-D fluid-thermal) as the element type for modeling with ANSYS (ANSYS, Inc., Canonsburg, PA). The property of the fluid material is set according to the properties of deionized (DI) water [i.e., $\text{density} = 1 \text{ kg/m}^3, \text{dynamic viscosity} = 1.002 \times 10^{-3}$ $(\text{N} \cdot \text{s} \cdot \text{m}^{-2})$, kinematic viscosity $= 1.004 \times 10^{-6} \text{ m}^2/\text{s}$]. The environmental air pressure is set to 1 atm. The environmental temperature is set to be 300 K. The boundary conditions are applied as follows: 1) The aqueous fluid (water) flows into the device with a velocity of 3 mm/s (left edge) and flows out of the device (right edge) with a velocity of 3 mm/s while the fluid velocity at the lateral walls (top and bottom edges) are set to 0 mm/s; 2) pressures at the air pillar openings are all set to 1 atm; and 3) the fluid velocity components normal to the air pillar opening circumferences are all set to zero. Fig. 7(a) and (c) shows the solved flow rate profiles for devices with different hole-patterns, while Fig. 7(b) and (d) shows the solved pressure profiles. The color bar under the 2-D model shows the scale of the relative physical quantities.

Fig. 7(a) and (b) shows that higher flow rates can be achieved in the channel with the aligned air pillar design. This would allow higher collection rates and rapid flushing of the system for subsequent experiments. A major disadvantage of this design is the dead spots [dark blue area in Fig. 7(a), where flow rate is zero] that occur between adjacent pillars. Analytes could be trapped between these two pillars, reducing collection efficiency and preventing analyte residues to be flushed out. Moreover, higher pressure on the inlet of the device might imply higher risk to reach the critical pressure difference [red area in Fig. 7(b)].
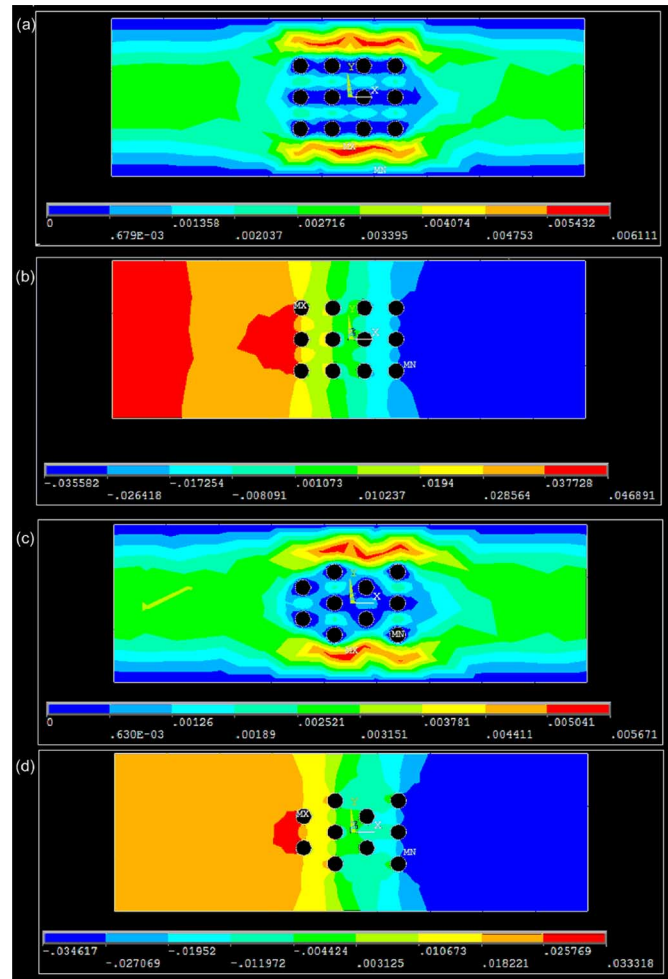

Fig. 7. Flow rate and pressure simulations of different air pillar hole patterns using ANSYS. (a) Flow rate profile of an aligned "holes matrix" pattern. (b) Pressure profile on an aligned "holes matrix" pattern. (c) Flow rate profile on an offsetting holes pattern. (d) Pressure profile on an offsetting holes pattern. The aqueous fluid (water) flows in the device with a velocity of 3 mm/s from the left edge of the layer and flows out from the right edge with a velocity of -3 mm/s, and the fluid velocity at the lateral walls are set to 0; fluid velocity components in directions normal to the circumferences of the air pillar openings are also set to 0. Pressures at the openings are all set to be equal to a standard air pressure.

This is the point at which the balance held by surface tension is broken, driving the fluid to occupy the space of the air pillars.

The offsetting pillar pattern [see Fig. 7(c) and (d)] shows that there exists a detectable flow rate through the entire pillar section of the channel. This flow would help optimize the performance of both the collection mechanism and flushing of the system. Hence, we choose the offsetting holes pattern for our device fabrication.

V. EXPERIMENTAL SETUP AND RESULTS

A. Nesslar's Reagent and Aerosolized Particles

1) Air Pillar Device: A single-level air pillar microfluidic channel device was placed in a sealed container with an inlet and an outlet for ammonia to provide the operation environment for the device. Nessler's reagent (NR), an aqueous liquid with no color, was infused at a rate of 15 μL/min through the channel of the air pillar device [see Fig. 8(a)]. A 30% ammonia solution was aerosolized by a nebulizer, and the vaporized NH_3 gas
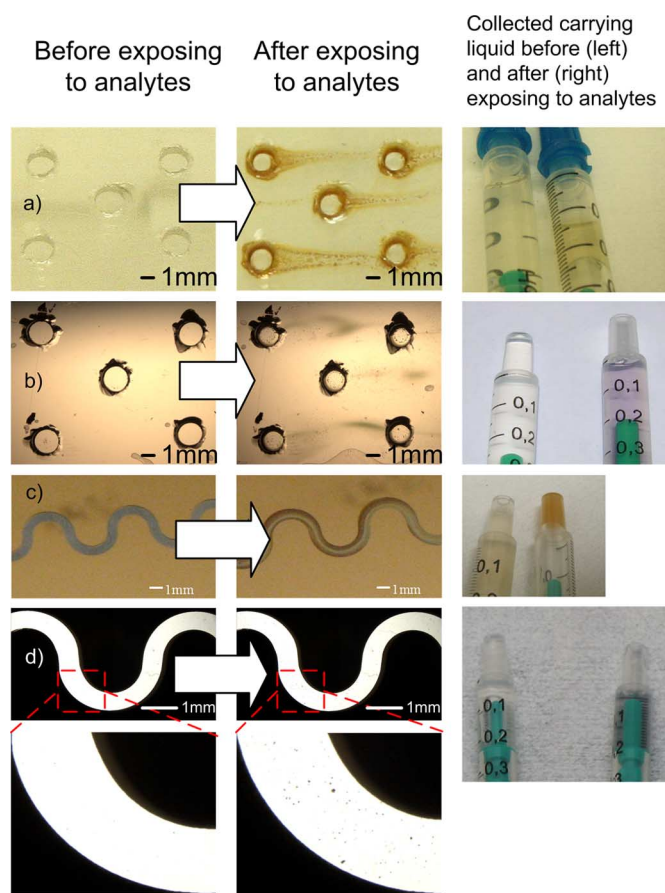
Fig. 8. Responses of collection devices to analytes, as well as collected liquid (in syringes) before (left) and after (right) exposure: (a) Air pillar device with NR flowing through the channel. It was then exposed to ammonia, and a color change from no color to rust brown occurred only a few seconds later. (b) Air pillar design with DI water flowing through the channel. The device was then exposed to aerosolized Kool-Aid. Color change to purple in the channel was observed. And the color change is more obvious by comparing the collected liquids. (c) Serpentine channel device with NR flowing through. Color in the channel changed to rust brown when the channel was exposed to gaseous ammonia. (d) Channel device with DI water flowing through the channel. The device was then exposed to aerosolized Kool-Aid. As shown in the zoomed-in area, particles appears in the flow after exposing to the analyte and the color changed to purple, as shown in the syringe containing the collecting liquids.
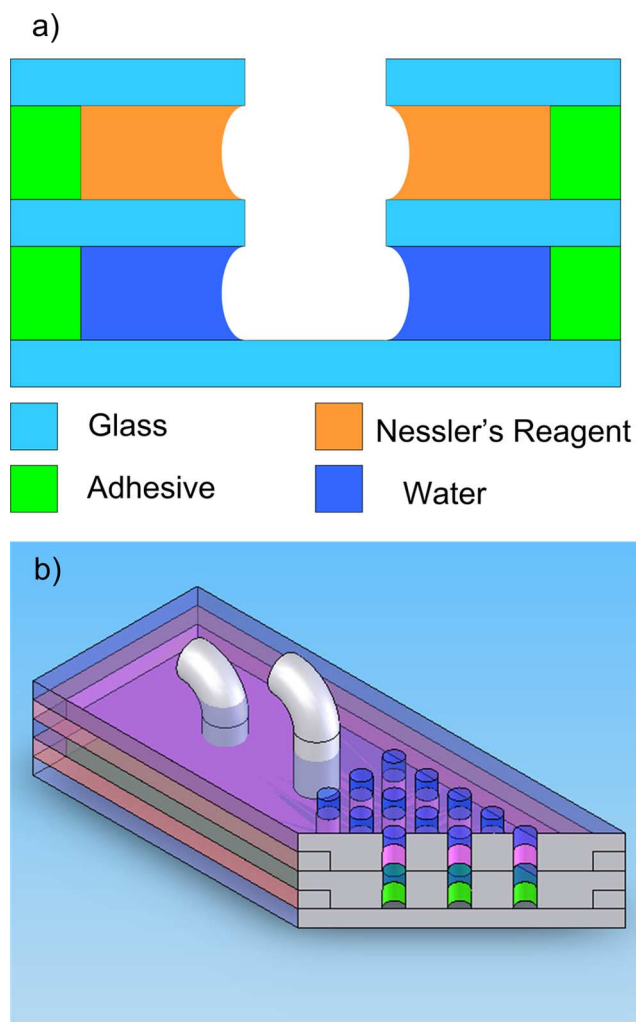

Fig. 9. Scheme of the two-layer air pillar device design. (a) Cross-sectional diagram of the two-layer device with aligned air pillars. (b) 3-D rendition of a multilayer air pillar device.

was pumped into the container. When NH_3 came in contact with NR, a rust brown substance, NH_4OH, was produced, indicating that NH_3 was collected into the channel at the gas–liquid interfaces of the air pillars [see Fig. 8(a)]. Syringes were connected to the outlet of the air pillar device during the whole ammonia application to collect the analyte-containing fluid for analysis afterward.

After that, Kool-Aid, a water soluble food product, was selected for the aerosolized particle test because of its ease of use and safety. The single-level air pillar device was filled with DI water (as the collecting liquid) at a rate of 15 μL/min [see Fig. 8(b)]. Kool-Aid was aerosolized with a nitrogen air gun and blown laterally over the device, allowing the particles to permeate the air pillar gas–liquid interfaces. The particles were collected by the dynamic DI water flow in the channel. These experiments show that with properly chosen collecting fluids, the device was able to collect both gaseous samples and solid particles.

2) Channel Device: As shown in the Fig. 8(c), the channel is flushed with NR at a rate of 15 μL/min after being placed in an open container. NH_3 from 30% ammonia solution was then vaporized into the container with a nebulizer. The color of the NR stream in the device then began to change to rust brown, from the side walls of the collecting fluid stream to the center of the stream.

Then, the same device was placed under a stereoscope and flushed with DI water at a rate of 15 μL/min [see Fig. 8(d)]. Kool-Aid was aerosolized and blown laterally toward the stream. The images in Fig. 8(d) show how particles were collected within the stream, proving that the device was able to collect both gaseous samples and aerosolized particles with proper collecting fluids.

3) Multilevel Air Pillar Device: A two-level air pillar device was placed in a sealed container with two inlets and an outlet. Fig. 9 shows a scheme of the device, indicating that different collecting fluid can be used in different levels for different analytes. In the experiment, the upper fluid level was NR and the lower level was DI water, and both were infused at a rate of 15 μL/min. Kool-Aid was introduced first and blown laterally with respect to the air pillars. The device response in Fig. 10(b) shows
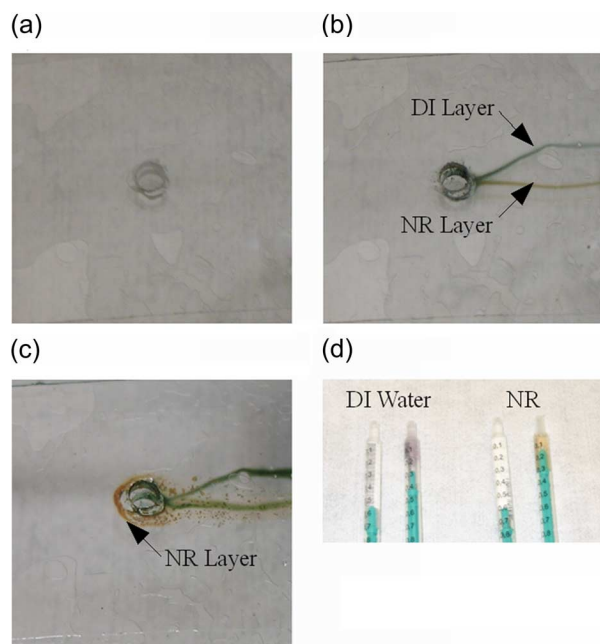
Fig. 10. Response of a two-layer air pillar device to different analytes. (a) Image of the two-level design with both DI water and NR (both limpid liquids) flowing through the system as the collection solvent. (b) Device was first exposed to the aerosolized Kool-Aid, which introduce a color change in both the DI water layer and the NR layer. (c) Device was then exposed to aerosolized ammonia from a nebulizer that caused the rust brown substance only in the NR layer. (d) Collected analyte-carrying collecting fluid from both layers: left: pre-exposure samples; right: postexposure sample.

that both fluids had the capacity to collect aerosolized particles. Then, NH_3 was vaporized by a nebulizer from 30% ammonia solution and introduced into the container through another inlet. The NH_3 reacted with the NR in the upper level to create the rust brown NH_4OH, as shown in Fig. 10(c). The collection process continued for 5 min, and adequate samples were gathered into syringes, as shown in Fig. 10(d).

B. Optimization of Collection Devices

To further increase the sensitivity of our devices, a straightforward method might be increasing the area of the gas–liquid interface. This optimization is expected to allow more analyte to be collected at a fixed time period, provided the same properties of the devices and the collecting liquid stream.

1) Channel Device: Two devices with different channel geometries were tested at the same time for a comparison. One channel design is a straight line with inlets at one end and outlets at the other; the other channel bears a design of a serpentine structure with five semicircle turns, as shown in Fig. 1 (top), which has a larger exposed surface area because of the increased channel length. Both devices were placed in a sealed container with an air inlet, an outlet, and an internal circulating fan. The container was then flushed with nitrogen to ensure an inertia pre-testing environment. The devices were then infused with DI water at a fixed rate of 10 μL/min, which was previously determined in order to prevent the balance of forces at the lateral gas–liquid interface from breaking. After the whole DI water-fluid channel was formed and confined by surface tension, a nebulizer was used for vaporizing from ammonia solution for 5 s and then both the inlet and outlet were sealed, and

the circulating fan turned on to enhance a uniform distribution of the gaseous NH_3. The NH_3 concentration in ammonia solution was carefully determined, so the amount of gaseous NH_3 was large enough to prevent the competition between the two devices, and small enough so the NH_3 concentration in the collecting DI water stream did not exceed the saturation concentration limit during the collecting process. Liquid streams carrying analyte were then conducted out from the outlet of the devices and then collected in 1-mL syringes for subsequent analysis.

The collected DI water liquid stream samples were then injected into ethyl vinyl acetate microbore tubings with a 1.5-mm diameter and a length of 7.5 cm. The 2-mm 76-gauge magnet wires were then inserted into each end of the tubing as probe tips, and the resistance is measured by a bench resistance meter. With the controlled amount of NH_3, higher concentrations of ions in the analyte-collecting liquid streams should result in higher conductivities, i.e., lower resistances.

The experimental results are shown in Table I. As we expected, since the serpentine channel design has an exposed gas–liquid interface area almost four times larger than the simple straight design, the analyte-carrying DI-water collected from the serpentine device has a lower resistance, indicating that it collects more analyte in a fixed time period comparing to the straight channel device.

2) Air Pillar Device: The air pillar devices were tested using the similar method as the channel devices. The only difference is that the flow rates of the air pillar design were able to be slightly higher, 15 μL/min, due to the robustness of the pinning effect at the edge of the holes.

A one-air pillar device, a five-air-pillar device, and a nine-air-pillar device were tested simultaneously. As expected, more air pillars imply larger gas–liquid interface area, thus larger ion collecting rate, and thus lower resistance.

C. Real-Time Sensing (Conductance Measurement) Using Air Pillar Device

A five-hole air pillar device was fabricated and then two 2-mm wire probes were inserted directly into the channel through the device inlet and outlet. The whole device was then placed in a chamber placed in a fume hood, and the probes were connected to a bench top resistance meter, measuring resistance of collecting fluid stream dynamically. DI water, the collecting liquid, was infused liquid, was infused through the device at a fixed rate of 15 μL/min during the experiment. Gaseous NH_3 was introduced using a nebulizer and further distributed into the chamber by a circulating fan and the upstream air flow from the fume hood. This environment allowed for constant flow of air over the device and provided a mimicry of real-world scenarios. After the device was flushed with DI water for 5 min, a baseline measurement was taken (liquid resistance -46 ± 0.5 MΩ). Then, the device is exposed to NH_3 vaporized from 30% ammonia solution. The transient change of resistance was recorded each 15 s until a quasi-static state was reached. Similar experiment was conducted for 15% and 7.5% NH_3. Between each experiment, the residue NH_3 was completely vented away, and the collecting liquid residue in the device was flushed by DI water for 5 min.

Fig. 11 shows how the device acted in response to the NH_3 concentration in environment. Decreasing the NH_3 by half

TABLE I
RESISTANCE OF DI WATER IN VARIOUS COLLECTION DEVICES AFTER EXPOSURE TO GASEOUS NH₃ AND THE AREA OF GAS–LIQUID INTERFACE IN DIFFERENT
DEVICES. DI WATER WAS FLOWED THROUGH EACH DEVICE AT A CONSTANT RATE, WITH AN IMPEDANCE OF 1.4 GΩ BETWEEN THE PROBES PLACED IN THE
MICROBORE TUBINGS. DIFFERENT DEVICES WERE THEN EXPOSED TO VAPORIZED NH₃ FOR SEVERAL MINUTES AT VARIOUS CONCENTRATION LEVELS

| Aqueous NH₃ Concentration	Conductance Measurements Comparison		
	Device Type	Surface Area(mm²)	Resistance
30%	1 Hole Air Pillar Device	0.12	60 MΩ
30%	5 Hole Air Pillar Device	0.53	51 MΩ
30%	9 Hole Air Pillar Device	0.95	44 MΩ
30%	Straight Gold Device	5	53 MΩ
30%	Serpentine Gold Device	9.5	46 MΩ
3.65%	1 Hole Air Pillar Device	0.12	240 MΩ
3.65%	5 Hole Air Pillar Device	0.53	191MΩ
3.65%	9 Hole Air Pillar Device	0.95	137 MΩ
3.65%	Straight Gold Device	5	173 MΩ
3.65%	Serpentine Gold Device	9.5	156 MΩ
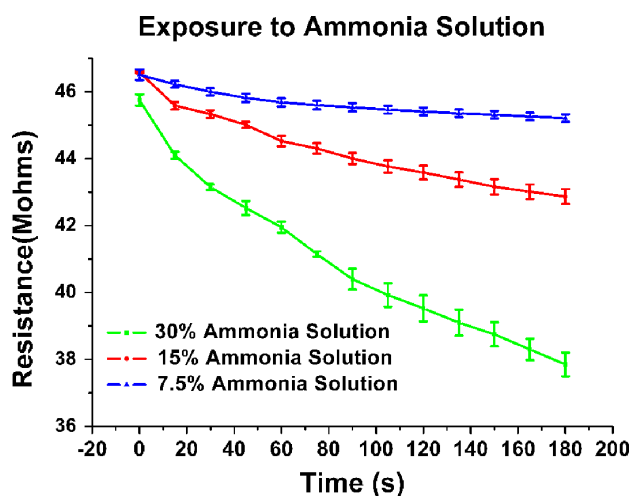
Fig. 11. Response of the air pillar collecting device exposing to gaseous NH₃. The five-hole air pillar device was infused with DI water stream at a rate of 15 μL/min and then exposed to different concentrations of ammonia solution. NH₃ was vaporized by a nebulizer at time 0 for each concentration.

would result in roughly a linear response of the resistance of the collecting liquid stream in the device. This demonstrates that the device is able to detect different concentrations of NH₃ in real time. The error bars on the detection curves demonstrate the reliability of the device. Only a simple and short discarding step is needed to prepare it for reacquisition and measurement.

VI. CONCLUSION AND FUTURE WORK

We have created devices with reliable liquid–air interfaces for aerosolized particle and gas collection (and detection), using different methods. The simplistic and inexpensive fabrication of these devices provides robustness and the potential to integrate them into practice detection systems. With liquid–air interfaces pinned at hydrophilic–hydrophobic SAM-gold–glass interfaces, we have demonstrated channel devices with lateral gas–liquid interfaces, and further optimized the channel structure to increase the exposing interface area to the environment analytes. We also demonstrated collecting devices utilizing air pillar structure to pin the liquid–gas interface at the edge of patterned holes. Because of the much simpler fabrication process and robust materials (i.e., no SAM thin film), these devices have much longer shelf life, lower cost, and better compatibility. Moreover, the capability of collecting different analytes in the environment simultaneously with different levels has been demonstrated by multilevel air pillar devices.

The potential of our devices for real-time collecting and analyzing of aerosolized or gaseous chemical and biological agents have also been demonstrated by both direct observation and measurement of the conductance of collecting liquid. However, further optimization would be necessary, and future works may include four aspects. First, for the channel devices, the quality of the surface treatment could be further improved, and more calculation and optimization is needed to further increase the exposed surface area, and to make a tradeoff between a higher flow rate (i.e., a high collecting rate) and a larger risk of wearing-out of the SAM (i.e., a shorter life for operating). Second, the air pillar structures can be expanded to multiple layers by stacking more glass slides with aligned holes. Third, in the gold channel structure, the analytes enter the stream from the lateral direction; while in the air pillar structure, the analytes enter the stream from the vertical direction. Hence, a

combination of the two structures is possible where the device collects analytes from both the lateral and vertical directions; the collecting efficiency is expected to be enhanced. Finally, with an accurate control module, and either structure as the core device, an automatic total analysis system-on-a-chip could be implemented, which would further demonstrate the commercial potential of our designs.

Acknowledgment

References

[1] B. Zhao, N. O. L. Viernes, J. S. Moore, and D. J. Beebe, "Control and applications of immiscible liquids in microchannels," *J. Amer. Chem. Soc.*, vol. 124, no. 19, pp. 5284–5285, 2002.

[2] J. Atencia and D. J. Beebe, "Controlled microfluidic interfaces," *Nature*, vol. 437, pp. 648–655, 2005.

[3] C. A. Pope, "Air pollution and health—Good news and bad," *N. Engl. J. Med.*, vol. 351, pp. 1132–1134, 2004.

[4] B. H. Timmer, K. M. van Delft, W. W. Koelmans, W. Olthuis, and van den Berg, "Selective low concentration ammonia sensing in microfluidic lab-on-a-chip," *IEEE Sensors J.*, vol. 6, no. 3, pp. 829–835, Jun. 2006.

[5] E. D. Lester and A. Ponce, "An anthrax 'smoke' detector," *IEEE Eng. Med. Biol. Mag.*, vol. 21, no. 5, pp. 38–42, Sep./Oct. 2002.

[6] T. Frisk, D. Rönnholm, W. V. D. Wijngaart, and G. Stemme, "A micromachined interface for airborne sample-to-liquid transfer and its application in a biosensor system," *Lab. Chip*, vol. 6, pp. 1504–1509, 2006.

[7] S. S. Sridharamurthy and H. Jiang, "A microfluidic device to acquire gaseous samples via surface tension held gas-liquid interface," *IEEE Sensors J.*, vol. 7, no. 9, pp. 1315–1316, Sep. 2007.

[8] J. Greenwood, D. Cheng, Y. Liu, and H. Jiang, "Air to liquid sample collection devices using microfluidic gas/liquid interfaces," *Proc. IEEE Sensors*, pp. 720–723, 2008.

[9] B. Zhao, J. S. Moore, and D. J. Beebe, "Principles of surface-directed liquid flow in microfluidic channels," *Anal. Chem.*, vol. 74, pp. 4259–4268, 2002.

[10] B. Zhao, J. S. Moore, and D. J. Beebe, "Surface-directed liquid flow inside microchannels," *Science*, vol. 291, pp. 1023–1026, 2001.

[11] A. Hibara, S. Iwayama, S. Matsuoka, M. Ueno, Y. Kikutani, M. Tokeshi, and T. Kitamori, "Surface modification method of microchannels for gas-liquid two-phase flow in microchips," *Anal. Chem.*, vol. 77, pp. 943–947, 2005.

[12] G. M. Whitesides, E. Ostuni, S. Takayama, X. Jiang, and D. E. Ingber, "Soft lithography in biology and biochemistry," *Annu. Rev. Biomed. Eng.*, vol. 3, pp. 335–373, 2001.

[13] D. Ryan, B. A. Parviz, V. Linder, V. Semetey, S. K. Sia, J. Su, M. Mrksich, and G. M. Whitesides, "Patterning multiple aligned self-assembled monolayers using light," *Langmuir*, vol. 20, pp. 9080–9088, 2004.

[14] G. T. Roman, M. Wang, K. N. Shultz, C. Jennings, and R. T. Kennedy, "Sampling and electrophoretic analysis of segmented flow streams using virtual walls in a microfluidic device," *Anal. Chem.*, vol. 80, pp. 8231–8238, 2008.

[15] Y. N. Xia, E. Kim, M. Mrksich, and G. M. Whitesides, "Microcontact printing of alkanethiols on copper and its application in microfabrication," *Chem. Mat.*, vol. 8, pp. 601–603, 1996.

[16] C. D. Bain and G. M. Whitesides, "Correlations between wettability and structure in monolayers of alkanethiols adsorbed on gold," *J. Amer. Chem. Soc.*, vol. 110, no. 11, pp. 3665–3666, 1988.

[17] Y. Y. Feng, Z. Y. Zhou, X. Y. Ye, and H. J. Xiong, "Passive valves based on hydrophobic microfluidics," *Sens. Actuators A*, vol. 108, no. 1, pp. 138–143, 2003.

[18] D. Cheng, Y.-J. P. Choe, and H. Jiang, "Controlled liquid-air interfaces and interfacial polymer micromembranes in microfluidic channels," *J. Microelectromech. Syst.*, vol. 17, no. 4, pp. 962–973, 2008.

Jason D. Greenwood received the B.S. degree in computer engineering from North Dakota State University, Fargo, and the M.S. degree in electrical engineering from the University of Wisconsin, Madison, in 2006 and 2008, respectively.

He is currently with the development team at International Business Machines, Rochester, MN, where he is engaged in research on next-generation processors to be used in super computing systems and gaming engines.
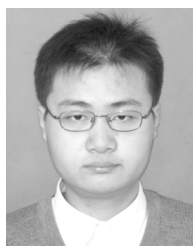
Ye Liu (S'08) received the B.S. degree in microelectronics from Peking University, Beijing, China, and the M.S. degree in electrical engineering from the University of Delaware, Newark, in 2006 and 2008, respectively. He is currently pursuing the Ph.D. degree at the Department of Electrical and Computer Engineering, University of Wisconsin, Madison.

His research interests include liquid microlenses, thermal wettability switches, and biosensors.

David E. Busacker received the B.S. degree in electrical engineering from the St. Cloud State University, St. Cloud, MN, in 2007 and the M.S. degree in electrical engineering from the University of Wisconsin, Madison, in 2009.

He is currently with Massachusetts Institute of Technology Lincoln Laboratory, Lexington, MA.

Daming Cheng received the B.S. and M.S. degrees in materials science and engineering from Tsinghua University, Beijing, China, in 2003 and 2005, respectively. He is currently pursuing the Ph.D. degree in materials science from the University of Wisconsin, Madison.

His current research interests include development of multiphase interfaces in microfluidic channels, interfacial polymerization of thin membranes with high aspect ratio, and biological and chemical sensing using liquid crystals.
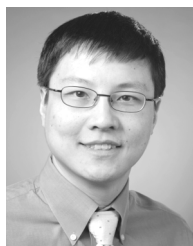
Hongrui Jiang (S'98–M'02–SM'10) received the B.S. degree in physics from Peking University, Beijing, China, and the M.S. and Ph.D. degrees in electrical engineering from Cornell University, Ithaca, NY, in 1999 and 2001, respectively.

He is currently an Associate Professor with the Department of Electrical and Computer Engineering, a Faculty Affiliate with the Department of Biomedical Engineering, and a Faculty Member of the Materials Science Program, University of Wisconsin, Madison. From 2001 to 2002, he was a Postdoctoral Researcher at the Berkeley Sensor and Actuator Center, University of California-Berkeley, Berkeley. His research interests include microfabrication technology, biological and chemical microsensors, microactuators, optical microelectromechanical systems, smart materials and micro-/nanostructures, lab-on-a-chip, and biomimetics and bioinspiration.

Dr. Jiang was the recipient of the National Science Foundation CAREER Award and Defense Advanced Research Project Agency Young Faculty Award in 2008.